Molecular mechanisms controlling synaptic recruitment of GluA4 subunit-containing AMPAreceptors

Luchkina, N.V., Coleman, S.K., Huupponen, J., Cai, C., Kivisto, A., Taira, T., Keinanen, K. and Lauri, S.E.

Molecular mechanisms controlling synaptic recruitment of GluA4 subunit-containing AMPA-receptors critical for functional maturation of CA1 glutamatergic synapses

Natalia V. Luchkina[1,2], Sarah K. Coleman[2], Johanna Huupponen[1,2], Chunlin Cai[2], Anna Kivistö[1], Tomi Taira[1,3], Kari Keinänen[2], and Sari E. Lauri[1,2]

[1]Neuroscience Center, [2]Department of Biosciences and [3]Department of Veterinary Biosciences, University of Helsinki, Finland
C.C.´s present address: Department of Pathophysiology, Anhui Medical University, Hefei, 230032, P.R. China

S.K.C.'s present address: Department of Life Sciences, University of Westminster, London, W1W 6UW, U.K.

Corresponding author:

Sari Lauri
Neuroscience Center and Department of Biosciences,
PO Box 65 (Viikinkaari 1), 00014 University of Helsinki, Finland
Email: sari.lauri@helsinki.fi

Abbreviated title: Molecular mechanisms of silent synapse activation (<50 characters)

Number of pages: 19

Number of figures: 5

Number of words for Abstract:146, Introduction: 314 Discussion: 1436

Conflict of Interest: The authors declare no competing financial interests

Abstract

Synaptic recruitment of AMPA receptors (AMPARs) represents a key postsynaptic mechanism driving functional development and maturation of glutamatergic synapses. At immature hippocampal synapses, PKA-driven synaptic insertion of GluA4 is the predominant mechanism for synaptic reinforcement. However, the physiological significance and molecular determinants of this developmentally restricted form of plasticity are not known. Here we show that PKA activation leads to insertion of GluA4 to synaptic sites with initially weak or silent AMPAR-mediated transmission. This effect depends on a novel mechanism involving the extreme C-terminal end of GluA4, which interacts with the membrane proximal region of the C-terminal domain to control GluA4 trafficking. In the absence of GluA4, strengthening of AMPAR-mediated transmission during postnatal development was significantly delayed. These data suggest that the GluA4-mediated activation of silent synapses is a critical mechanism facilitating the functional maturation of glutamatergic circuitry during the critical period of experience-dependent fine-tuning.

Key words : AMPA –receptor, GluA4, silent synapse, development, synaptic targeting

Highlights

- PKA activation leads to synaptic unsilencing via insertion of GluA4
- This depends on a novel mechanism involving the extreme C-terminal end of GluA4
- Absence of GluA4 causes delayed postnatal maturation of AMPA transmission

Introduction

GluA4 AMPAR subunit is transiently expressed in hippocampal pyramidal neurons during the first postnatal week, which corresponds to the time of activity-dependent fine-tuning of glutamatergic synaptic connectivity. This involves strengthening and stabilization of immature synapses via both presynaptic and postsynaptic mechanisms. The regulated insertion of AMPA receptors to weak or functionally silent synapses is thought to be a key postsynaptic mechanism underlying experience-dependent maturation of transmission (Kerchner and Nicoll 2008; Hanse et al., 2013).

A suggested model for activity-dependent synaptic recruitment of AMPARs involves insertion of receptors to extrasynaptic areas followed by lateral diffusion to synaptic sites and capture within the postsynaptic density (PSD) (Opazo and Choquet, 2011). However, early in development, spines, which would limit lateral diffusion, are mostly absent (Fiala et al., 1998) and the molecular composition of the postsynaptic density (PSD) is distinct from the adult (Elias et al., 2006; Bassani et al., 2013). Consequently, the detailed molecular mechanisms underlying AMPAR and, in particular, GluA4 trafficking at immature synapses are not completely understood. Similar to other types of ionotropic glutamate receptors, synaptic recruitment of GluA4-containing AMPARs is regulated by interactions mediated by its C-terminal domain (CTD; Zhu et al., 2000; Boehm et al., 2006; Luchkina et al., 2014), which is a target for phosphorylation by PKA (Carvalho et al., 1999, Esteban et al., 2003). At GluA4 expressing developing synapses, PKA activation is both necessary and sufficient to drive AMPA receptors to synapses and to produce long-term potentiation (LTP) of synaptic transmission (Zhu et al., 2000; Esteban et al., 2003; Yasuda et al., 2003; Luchkina et al., 2014). This form of plasticity is restricted to early development (the first postnatal week in rodents), after which LTP becomes dependent on multiple kinases and, in particular, Ca^{2+}/calmodulin dependent kinase II (CaMKII; e.g. Yasuda et al., 2003). Here we have examined the molecular mechanism and physiological significance of the immature type GluA4-PKA dependent LTP.

Materials and methods

Animals

Experiments were performed on 4- to 6-day-old Wistar rats and 4- to 34-day-old wild-type (WT) or GluA4−/− mice kindly provided by Hannah Monyer (University of Heidelberg, Heidelberg, Germany; Fuchs et al., 2007). All experiments were done in accordance with the University of Helsinki Animal Welfare Guidelines.

Slice preparation

Animals were rapidly decapitated, and the brains were quickly removed from the skull and submerged in ice-cold dissection solution containing 124 NaCl, 3 KCl, 1.25 NaH_2PO_4, 10 $MgSO_4$, 26 $NaHCO_3$, 15 D-glucose, and 1 $CaCl_2$ and equilibrated with carboxygen (5% CO_2 + 95% O_2). Parasagittal hippocampal slices (350–400 μm) were cut with a vibratome (Leica Microsystems, Wetzlar, Germany) in dissection solution and placed in a recovery chamber, submerged in solution containing the following (mM): 124 NaCl, 3 KCl, 1.25 NaH_2PO_4, 3 $MgSO_4$, 26 $NaHCO_3$, 15 D-glucose, and 2 $CaCl_2$ (bubbled with carboxygen). To prevent recurrent excitation, the CA3 region was cut away in experiments where evoked EPSCs were recorded.

Electrophysiology

After 1–5 hour storage in a recovery chamber, an individual slice was transferred to a recording chamber where it was constantly perfused with oxygenated ACSF containing (mM): 124 NaCl, 3 KCl, 1.25 NaH_2PO_4, 1 $MgSO_4$, 26 $NaHCO_3$, 15 D-glucose, and 2 $CaCl_2$ (at 30°C). Electrophysiological experiments were performed on CA1 pyramidal cells under visual guidance using a MultiClamp 700A amplifier (Molecular Devices, Sunnyvale, CA, USA) in whole-cell voltage-clamp mode. The electrodes were 3–5 MΩ and contained the following (mM): 130 $CsMeSO_4$, 10 HEPES, 0.5 EGTA, 4 Mg-ATP, 0.3 Na-GTP, 5 QX-314, and 8 NaCl (278±5 mOsm, pH 7.2–7.4). Uncompensated series resistance (<30 MΩ) was monitored throughout experiments, and recordings were interrupted if it changed by >20%. Evoked EPSCs were elicited by Schaffer collateral pathway stimulation with a bipolar electrode in the presence of $GABA_A$-receptor antagonist picrotoxin (100 μM). For mEPSCs recordings, 1mM TTX was also included. Baseline stimulation frequency was 1/20 s or 1/15 s and the intensity was adjusted to the minimum strength eliciting a stable response and, for experiments estimating AMPA/NMDA ratio, with an average amplitude in the range 20–50 pA. To activate only a few presynaptic fibers, a minimal stimulation protocol was employed. Briefly, the stimulus intensity was set so that a 25% change did not affect response amplitude or failure rate and failures were observed in about 50% of the time (Stevens and Wang, 1995; Isaac et al., 1996). Synaptic transmission was elicited at low frequency 1/15 s to avoid frequency-dependent synaptic depression (Saviane et al., 2002; Voronin and Cherubini, 2004). Pharmacological compounds were obtained from Tocris Bioscience (Bristol, UK) and Abcam (Cambridge, UK). Forskolin was applied in <15 min after obtaining whole cell access.

The relevant purified GST-fusion proteins or GST were prepared as described (Coleman et al., 2010). Aliquots of all the protein constructs were run on gel and stained with Coomassie Blue to confirm the

correct size and integrity of the protein. The proteins were dialysed against a buffer containing (mM): 130 $CsMeSO_4$, 10 HEPES, 0.5 EGTA and 8 NaCl (pH 7.2–7.4) and included in the intracellular solution at a concentration of 0.5 µM. Interleaved control experiments with GST and/or an effective GST-A4 CTD construct were done to control intracellular dialysis and peptide diffusion into the recorded cell. Encoded residues were GluA4(835–902) for complete GluA4 CTD (based on numbering of the full polypeptide sequence, UniProt P19493). The GluA4 CTD mutations encoded the residues; GluA4(870–902), GluA4(835–869), GluA4(835-901), GluA4(835-896), GluA4(835–901; L901A), GluA4(835–902; S862A), GluA4(835–902; S862D), GluA4(835–902; R841S, K845S, R846S). Mutations were generated by PCR and standard molecular biological techniques and were verified by sequencing.

WinLTP 2.01 program (Bristol, UK; Anderson and Collingridge, 2001) was used for data acquisition. Spontaneous events were detected using the Mini Analysis Program 6.0.7. (Synaptosoft, Decatur, GA, USA). The amplitude threshold was set to 4–5 times of the baseline RMS (root mean square) noise level and the all detected events were verified visually. Evoked synaptic responses were analyzed using WinLTP. The amplitude of AMPA currents at –70 mV was measured as the peak relative to the average baseline level before stimulation, for NMDA currents at +40 mV 50–60 ms after stimulation. Decay time of the AMPA currents was calculated from 90-37% of the peak amplitude using the Mini Analysis Program 6.0.7. In experiments, where minimal stimulation was used, the amplitude threshold for identification of responses vs. failures at both –70 and +40 mV was set to 2 times of the RMS noise level at +40 mV due to the higher noise level at this potential, all responses were verified visually and were invariant in shape. For time course plots, detected events were calculated in 60 s or 120 s bins and normalized to the baseline level. For the histograms, data are presented as percentage of last 10 min of the relevant dataset after drug application relative to the baseline level.

Cell culture, DNA constructs and transfection

Primary hippocampal neurons were obtained from E17 mouse embryos and provided weekly by University facilities. Cells were dissociated and plated at a density of 50 000 cells/cm^2 on poly-D-lysine-coated Æ 12mm round glass coverslips in 24-well plates in glial cell-conditioned B27-supplemented Neurobasal medium (Life Technologies, Carlsbad, CA, USA). The cells were transfected on day 10 *in vitro* (DIV10) by using calcium phosphate method (Li et al., 2007). The medium was changed to pre-warmed Neurobasal (no supplements) containing 10 mM $MgCl_2$ (transfection medium) 1 h before transfection. For each well, a total of 35 µl contained: 2 µg plasmid DNA, 0.25 M $CaCl_2$ mixed with 17.5 µl of 2xHEPES-buffered saline (pH 7.06; 42 mM HEPES, 274 mM NaCl, 10 mM KCl, 1.4 mM Na_2HPO_4, 15 mM D-glucose); transfection mixture was added dropwise to cells. Cells were incubated at 37°C in 5% CO_2 for 4 hours. After a fine precipitation formed, cells were washed with transfection medium 2–3 times. Thereafter, it was replaced with the original glial-conditioned culture medium. The cells were analyzed 5–7 days later (DIV 15–17).

Constructs used for transfection were based on the N-terminally eGFP-tagged rat GluA4 (UniProt P19493; flip isoform) where full-length construct encoded residues 22–902 (residues 1–21 encode a signal peptide). The encoded residues in GFP-GluA4 mutants were: GFP-A4(22–896), GFP-A4(22–837,

870–902), GFP-A4(22–902; R841S, K845S, R846S). Mutations were generated by PCR and standard molecular biological techniques. All constructs and mutations were verified by sequencing the entire PCR amplified region.

Immunofluorescence staining and confocal microscopy

For surface immunostaining of GFP constructs, anti-GFP antibodies (1:1000, Abcam, Cambridge, UK) were added into each well and incubated for 30 min at room temperature. Then hippocampal neurons were washed in PBS (2x10 min) and fixed in 4% paraformaldehyde in PBS for 20 min, rinsed with PBS (2x10 min), and permeabilized in 0.2 % Triton-X-100 in PBS for 10 min. The cells were then incubated for 2 h with 4% bovine serum albumin (BSA), 3% normal goat serum (NGS), 0.05% gelatin and 0.2% Triton X-100 (blocking solution; in PBS) and left overnight at +4 °C with the primary antibodies/antisera in the blocking solution. For co-localisation studies, anti-PSD95 monoclonal antibody (1:1000; 75-028, NeuroMab, Davis, CA, USA) were used. In some cases anti-MAP2 mouse monoclonal antibodies (1:500, Sigma-Aldrich, St. Louis, MO, USA) were used as a dendritic marker. The stained cells were washed with 0.2% Triton X-100/PBS (1x10 min) and with PBS/1%BSA/1%NGS (2x10 min) and incubated with appropriate Alexa Fluor 405 (blue)- and Alexa Fluor 568 (red)-conjugated secondary antibodies (1:500, Life Technologies, Carlsbad, CA, USA). After cells were mounted in Fluoromount™ Aqueous Mounting Medium (Sigma-Aldrich, St. Louis, MO, USA), images were acquired as z stacks using the x63 objective 0.7× mechanical zoom at optimal resolution in Zeiss LSM 710 confocal microscope.

Image analysis

Images were collapsed to maximal projection and analyzed in Matlab with SynD (Schmitz et al., 2011). Background fluorescence was measured in a region without cells and subtracted prior to analysis in ImageJ (Schneider et al., 2012). Synapses were detected based on the staining for PSD95. Detected regions were subsequently used to measure the synaptic intensity of GFP-A4 constructs. Mean fluorescent intensity of the soma was calculated by averaging the intensity from 10 regions of interest (ROIs) placed in the soma. Synaptic recruitment was estimated as the ratio of the mean intensity at synapses to mean somatic intensity, while dendritic delivery – as mean dendritic intensity (including synaptic and extrasynaptic regions) to mean somatic intensity.

Statistical analysis

All the error bars represent the standard error of the mean (SEM). Statistical significance has been assessed using ANOVA or Student's two tailed t-test in SigmaPlot 11 (Systat Software, San Jose, CA, USA) or IBM SPSS Statistics (IBM Corporation, North Castle, NY, USA). If the assumption of normal distribution of the residuals failed, random permutation tests for ANOVA were performed in R software (R Core Team, 2014). The age-dependence of AMPA/NMDA ratio was tested using simple linear regression analysis (method of least squares). $p<0.05$ was considered as statistically significant.

Results

PKA activation leads to synaptic unsilencing via insertion of GluA4

We recently showed that forskolin application leads to an increase in both the amplitude and frequency of miniature EPSCs (mEPSCs) at immature CA1 pyramidal neurons, due to PKA-dependent mobilization of GluA4 (Luchkina et al., 2014). The observed increase in mEPSC frequency suggests activation of postsynaptically silent synapses via insertion of GluA4. To characterize this effect in more detail, we used minimal stimulation to record inputs with an initially low success rate (<0.5) of AMPAR-mediated EPSCs in the neonatal (P4-P8) CA1 pyramidal neurons in both wild type (WT) and GluA4-/- mice (Fuchs et al., 2007). The AMPAR-mediated component of the EPSC was recorded at a holding potential of -70mV in the presence of picrotoxin (PiTX) to block fast GABAergic inhibition, while the NMDAR-mediated component was recorded at +40 mV and isolated based on its slow kinetics. In 6 out of 9 WT cells, the success rate of AMPAR-mediated EPSCs was significantly lower as compared to NMDA (0.18±0.03 for AMPA, 0.40±0.09 for NMDA; n=6; p<0.01), indicative of postsynaptically silent synapses. Interestingly, no significant difference between AMPA and NMDA success rates were detected in any of the recorded cells in GluA4 -/- mice (n=9), suggesting that lack of GluA4 affected the proportion of silent inputs in the synapse population. Furthermore, the basal potency of AMPAR mediated EPSCs but not NMDAR-mediated EPSCs were higher in GluA4-/- as compared to WT (p<0.05; Fig. 1B vs Fig. 1A), while no statistically significant difference in the AMPA or NMDA success rate was detected between the genotypes.

In the WT mice, extracellular application of forskolin (50 µM) led to a significant increase in the amplitude of AMPA-receptor mediated EPSCs, due to an increase in both potency (192±29 %, n=9, p<0.05) and success rate (265±54 %, n=9, p<0.01; Fig. 1A). A single example of a synapse showing weak or subthreshold AMPA receptor mediated transmission but a visible NMDA-receptor mediated EPSC under basal conditions, and robust upregulation of AMPA currents upon forskolin application is depicted in the figure 1A (top panel). No changes in the NMDAR-mediated transmission in response to forskolin application were detected (potency: 98±10 %, p=0.73; success rate: 109±17 %, p=0.89; Fig. 1), suggesting that presynaptic efficacy was not significantly altered and further, that the potentiation of EPSCs was most likely driven by postsynaptic insertion of AMPA receptors. In contrast, forskolin had no effect on the potency of AMPA and NMDA EPSCs in the GluA4-/- mice (99±13 % and 104±17 %, respectively). A small non-significant increase in the success rate of both AMPA and NMDA EPSCs was observed, presumably mediated by some compensatory presynaptic mechanism (AMPA: 148±36 %; NMDA: 195±75 %, p=0.39; Fig. 1B).

These data together with our previous results (Luchkina et al., 2014) show that PKA activation leads to insertion of GluA4 to immature synapses with initially weak or silent AMPA transmission.

Maturation of AMPAR-mediated transmission is perturbed in the absence of GluA4

During the first two weeks of development, the relative contribution of AMPARs to postsynaptic currents increases (Crair and Malenka, 1995; Durand et al., 1996; Hsia et al., 1998; Lu et al., 2001; Ye et al., 2005). To study the role of GluA4 in the AMPAfication of the glutamatergic synapses, we analyzed the amplitude ratio of the AMPAR- vs. NMDAR-mediated EPSCs in WT and GluA4-/- mice at different developmental stages (Fig. 2A). A significant correlation of AMPA/NMDA ratio with age during first two weeks of development was observed in WT mice (linear regression analysis: r^2=0.34 for P4 to P15, p<0.001, n=41), but not in GluA4-/- mice (r^2=0.03, p=0.24, n=45). At P6-P8 (WT n=17, GluA4 -/- n=19) and at P14-15 (WT n=9, GluA4 -/- n=11), the AMPA/NMDA ratio was significantly smaller in the GluA4 -/- mice as compared to the WTs (p<0.05; Fig. 2B). In GluA4-/- mice, a steep increase in AMPA/NMDA ratio was observed between P14 and P18 (Fig. 2A, B), a developmental stage when the ratio was already stabilized to apparent adult levels in the WT mice. Finally, no significant differences in the AMPA/NMDA ratio between the genotypes were detected at P16-P34.

Homomeric GluA4 AMPA receptors and in particular, the GluA4 'flop' splice variants show faster kinetics as compared to other types of AMPARs (Mosbacher et al., 1994; Geiger et al., 1995; Zhu, 2009), which may affect the amount of depolarization at postsynaptic neurons in response to receptor activation. The decay time of AMPA EPSCs increased during development in both WT and GluA4-/- mice (p<0.001); however, no significant differences in the kinetics of the AMPA EPSCs were detected between the genotypes at any stage of development (P4-P5: WT 4.2±0.6 ms, GluA4-/- 4.6±0.4 ms; P6-P8: WT 5.6±0.7 ms, GluA4-/- 5.7±0.8 ms; P14-P15: WT 10.5±0.8 ms, GluA4-/- 9.6±0.8 ms; P16-P34: WT 9.3±0.9 ms, GluA4-/- 10.2±0.5 ms). This result is consistent with predominant expression of GluA4 'flip' during early development (Monyer et al., 1991). Additionally, the data suggest that the observed developmental increase in the decay time of AMPA EPSCs depends on mechanisms that operate in the absence of GluA4, such as alternative splicing (Monyer et al., 1991), heteromerization with GluA2 (Kumar et al. 2002, Ho et al. 2007) or increased dendritic filtering (Hausser and Roth, 1997).

To study whether the delayed AMPAfication of synapses in the GluA4-/- mice was reflected in the overall development of glutamatergic input to CA1 neurons, we recorded action potential-independent spontaneous EPSCs (mEPSCs) from CA1 pyramidal neurons. Previously, no differences in mEPSCs were detected between WT vs. GluA4-/- mice at P4-P6 (Luchkina et al., 2014). Here we extended this analysis to P10-P11, but again found no significant differences in either frequency or amplitude of mEPSCs between the genotypes in the CA1 pyramidal neurons (WT: 28.5±5.2 events/min, 13.5±0.9 pA (n=8), GluA4-/-: 34.3±4.9 events/min, 14.1±1.0 pA (n=12) (Fig. 2C). Together, these data suggest that glutamatergic input to CA1 pyramidal neurons develops in the absence of GluA4, but the strengthening of AMPAR-mediated transmission relative to NMDAR is developmentally delayed.

The membrane proximal region of GluA4 CTD is critical for PKA-dependent synaptic potentiation

Having established that the PKA-dependent synaptic insertion of GluA4 is physiologically significant for silent synapse activation and maturation of AMPAR-mediated transmission, we went on to study the molecular mechanism behind this effect. Synaptic trafficking of GluA4 is mainly controlled by interactions mediated by its cytoplasmic tail, as scavenging any endogenous interactions by overexpressing the CTD interferes with its synaptic delivery (Zhu et al., 2000). Consistently, the effect of forskolin on EPSC amplitude at immature CA1 is strongly and selectively blocked when a GST fusion protein containing the full CTD of GluA4 (GST-A4(835-902)) is included in the intracellular solution (Luchkina et al., 2014). The GluA4 CTD has previously shown to interact with protein 4.1N (Coleman et al., 2003), PKCγ (Correia et al., 2003), α-actinin-1 and IQGAP1 (Nuriya et al., 2005), and it contains PKA / PKC phosphorylation site at Ser862 (Zhu et al., 2000; Gomes et al., 2007)(Figure 3A). In order to delineate in more detail the regions in GluA4 responsible for the blocking effect and to gain insight into the identity of the critical CTD interacting proteins, we used GST-A4 CTD fusion proteins with amino acid deletions or selective point mutations (Fig. 3A).

Various GST-fusion proteins containing the CTD sequences of the GluA4 were infused into cells at a concentration of 0.5 mM via the patch electrode while monitoring their effects on AMPAR–mediated evoked EPSCs. Interleaved control experiments with GST ensured that intracellular GST perfusion was not affecting forskolin – induced potentiation of EPSCs (2.64±0.39, n=11, p<0.001; not shown). GST–A4(835-869), containing the membrane proximal region (MPR) of the CTD, fully blocked forskolin-induced potentiation of EPSC (1.20±0.15, n=12, p=0.35; Fig. 3B). In contrast, GST-A4(870-902), containing the C-terminal half did not block potentiation (2.40±0.31, n=6, p<0.001; Fig. 3B), suggesting a critical role for the MPR in the synaptic recruitment of GluA4.

The MPR contains known interaction sites for protein 4.1N (Coleman et al., 2003) and PKCg (Correia et al., 2003), both implicated in surface expression of GluA4. To test the role of these proteins in forskolin-induced trafficking of GluA4, we next tested a GST–A4(835-902;RKR/SSS) fusion protein where Arg841, Lys845 and Arg846, the amino acid residues critical for binding to 4.1N and PKCg, are disrupted (Coleman et al., 2003). Inclusion of the RKR/SSS mutant to the patch pipette fully blocked the ability of forskolin to enhance EPSC amplitude (1.10±0.23, n=10, p=0.76; Fig. 3C), similarly to the wild-type protein. Thus, suggesting that these interactors alone are not important for the forskolin induced synaptic insertion of GluA4

Of the remaining protein interactors reported for GluA4 CTD (a-actinin-1 and IQGAP1; Nuriya et al., 2005), the exact sequence requirements are not known. However, it has been reported that phosphorylation of Ser862 strongly inhibits interaction of GluR4 with a-actinin-1 but has little effect on its interaction with IQGAP1 (Nuriya et al., 2005). Therefore we also tested GST–A4 CTD proteins where the serine 862 was mutated to prevent (S862A) or mimic (S862D) phosphorylation. Both GST–A4(835-902;S862A) and GST–A4(835-902; S862D) were able to block forskolin-induced potentiation of EPSC to the similar extent as the wild type GST-A4 CTD (1.27±0.23, n=9, p=0.3 and 0.99±0.17, n=7,

p=0.88, respectively; Fig. 3C). The lack of importance of phosphorylation status suggests that an a-actinin-1 interaction alone cannot explain PKA-dependent synaptic recruitment of GluA4-containing AMPARs at immature hippocampal neurons.

Extreme C-terminal sequences of GluA4 are involved in PKA-dependent synaptic potentiation

The other AMPA receptor subunits (GluA1-A3) contain a C-terminal PDZ binding motif critical for their synaptic trafficking (e.g. Hayashi et al., 2000; Malinow and Malenka, 2002; Anggono and Huganir, 2012). In GluA4, this PDZ binding motif is masked by an extreme C-terminal proline residue, and so far no proteins have been identified to bind this region *in vivo* (Coleman et al., 2010). Interestingly, we found that GST–A4(835-896), where six C-terminal amino acids were deleted, had no effect on forskolin-induced synaptic potentiation in neonatal CA1 (3.10±0.57, n=6, p<0.001; Fig. 3D). Changing the last two amino acids (GST-A4 CTD(835-901;L901A) was sufficient to render the A4 CTD unable to block the potentiation (forskolin induced potentiation 2.25±0.25, n=7, p<0.01; Fig. 3D), while a construct where the only the last proline was removed (GST-A4 CTD(835-901) was still able to inhibit forskolin-induced potentiation (1.22±0.13, n=7, p>0.13; Fig. 3D). These data show that similar to other AMPAR subunits, the C-terminal region of GluA4 has a critical role in its synaptic trafficking. However, as the C-terminal half of GluA4 CTD (GST-A4(870-902)) had no effect on the forskolin induced potentiation on its own (Fig. 3B), any effects of the extreme C-terminal end on PKA-induced GluA4 trafficking require the membrane proximal region.

Extreme C-terminal sequences regulate synaptic targeting and surface expression of GluA4 in hippocampal neurons

To further understand the molecular mechanisms of GluA4 trafficking, we studied the neuronal distribution of GFP-tagged GluA4 subunits where the CTD amino acids identified as critical for PKA-dependent synaptic plasticity (i.e. the MPR or extreme C-terminal region) were deleted. The GFP-A4(22-902; RKR/SSS) with mutated 4.1N/PKCg interaction site was also included, because of the previous evidence suggesting involvement of this region in GluA4 surface expression (Coleman et al., 2003; Boehm et al., 2006).

The subcellular distribution of the overexpressed constructs was first evaluated by comparing the GFP signal on confocal images to MAP2 staining that visualizes the full dendritic tree. Both wild type GFP-A4(22-902) and GFP-A4(22-902; RKR/SSS) contructs were strongly expressed along the dendrites. The intensity of GFP-A4(22-896) lacking the extreme C-terminal amino acids was apparently strongest in the soma, although dendritic expression was detectable. In contrast, GFP-A4(22-837; 870-902) lacking the MPR was completely restricted to the cell soma and was not detectable in the cell surface (mean intensity of the surface stain / mean GFP intensity at the cell soma 0.25±0.08, n=7, p<0.01 compared to the wild type GFP-A4(22-902) 0.96±0.10, n=11; not shown) (Fig. 4A). As this construct was not transported to dendrites, it could not be used for further analysis of this region in dendritic delivery and synaptic trafficking.

Quantification of the dendritic distribution confirmed no differences in relative dendritic intensity (mean intensity of GFP signal in dendrites / soma) between GFP-A4 and GFP-A4(22-902; RKR/SSS) constructs (Fig. 4B, C). In contrast, the intensity of GFP-A4(22-896) in the dendrites was significantly lower as compared to the full-length GFP-A4 (Fig 4B, C).

Synaptic recruitment of the constructs was evaluated based on their colocalization with PSD95 immunopositive puncta. GFP-A4 and GFP-A4(22-902; RKR/SSS) were clearly detected in the spine-like protrusions and co-localized with PSD95 (Fig. 4B). Surface staining suggested that the subunits were readily transported to the cell surface, consistent with the findings that spontaneous activity is sufficient for surface delivery of GluA4 (Zhu et al., 2000). Quantification of synaptic delivery (mean GFP intensity in PSD95 immunopositive regions / mean intensity at the soma) revealed no differences between wild type GFP-A4 and GFP-A4(22-902; RKR/SSS). Also the relative intensity of synaptic surface expression (GFP surface staining intensity in PSD95 immunopositive regions / PSD95 intensity) was similar for these two constructs (Fig. 4B, C). In contrast, both synaptic recruitment and relative synaptic surface staining of GFP-A4(22-896) were significantly smaller as compared to the wild type GFP-A4 (Fig. 4B, C), indicating a role for the extreme C-terminal sequences in synaptic targeting of GluA4.

Discussion

We have previously shown that expression of GluA4 at immature synapses is sufficient to switch the signaling requirements of LTP, by providing a PKA-dependent mechanism to strengthen AMPAR-mediated transmission (Luchkina et al., 2014). Here, we extend these findings to show that the PKA-driven synaptic insertion of GluA4 depends on unexpected molecular interactions of the extreme C-terminal end of GluA4. Our data further suggest that this mechanism contributes to silent synapse activation at the developing CA3-CA1 circuit to expedite maturation of AMPAR-mediated transmission.

Physiological significance of GluA4-dependent plasticity in developing glutamatergic circuitry

Silent synapses are a characteristic feature of immature neuronal circuits in various areas of the brain (Kerchner and Nicoll, 2008; Hanse et al., 2013). Trafficking of AMPA receptors is critical for postsynaptic unsilencing, however, less is known about the relative contribution of various endogenously expressed AMPAR subunits to this process. Using minimal stimulation, we show that PKA-activation induces functional GluA4 AMPA receptors at synapses with initially sub-threshold or silent AMPAR-mediated currents. In WT, but not GluA4 -/- mice, application of forskolin led to a significant increase in the potency and success rate of AMPAR-mediated EPSCs without significantly affecting NMDAR-mediated EPSCs. The most parsimonious explanation for these results is that PKA activation increases number or conductance of GluA4-containing AMPA receptors at previously

undetected release sites. Insertion of homomeric GluA4 receptors with higher single channel conductance (Swanson et al., 1997) to silent and/or labile synapses may also contribute to the observed increase in AMPA potency.

Silent synapse activation is thought to be critical for strengthening of AMPA transmission during development (Kerchner and Nicoll, 2008; Hanse et al., 2013). In support of a possible role of GluA4-dependent plasticity in silent synapse activation, the relative strength of AMPAR-mediated transmission (AMPA/NMDA ratio) was lower in GluA4-/- mice as compared to WTs during the second and third week of postnatal development (P6-P18), corresponding to the period of intense AMPAfication of transmission at WT CA3-CA1 synapses. However, in line with a previous report (Sagata et al., 2010) no differences in the AMPA/NMDA ratio between the genotypes were detected later on in development, indicating that strengthening of AMPAR-mediated transmission can progress in the absence of GluA4, but with a slower time course.

Intriguingly, during the first days of life (P4-P5), the AMPA/NMDA ratio was higher in the GluA4-/- mice as compared to WTs. Also, while the success rate of AMPA EPSCs was lower than NMDA EPSCs in WT mice, indicative of postsynaptically silent synapses within the activated synapse population, no corresponding difference was observed in GluA4 -/- mice at this developmental stage (P4-P8). One possible explanation is that GluA4 also contributes to the depression of AMPAR-mediated transmission in response to asynchronous activity at very young synapses (Xiao et al., 2004; Hanse et al., 2009). Thus, the absence of GluA4 may result in premature stabilization of AMPAR-mediated transmission at certain synapses.

Excitation/inhibition balance at immature networks is heavily regulated via various homeostatic and compensatory mechanisms (e.g. Huupponen et al., 2007). Also several mechanisms to counterbalance impaired Hebbian plasticity exist (Granger et al., 2013). From this perspective, it is not surprising that, in the absence of GluA4, no dramatic defects in overall circuit development were detected; no differences in either mEPSC frequency or amplitude were observed in CA1 pyramidal neurons between WT and GluA4-/- mice. Indeed, we previously found that in the absence of GluA4 an adult–type CaMKII-dependent LTP is observed already at P5-P8, suggesting that compensatory mechanisms are recruited to drive development of glutamatergic circuitry in the absence of GluA4. Thus, while not indispensable, the PKA-dependent insertion of GluA4 acts to facilitate the unsilencing and reinforcement of AMPAR-mediated transmission at immature synapses during network development.

Premature, or delayed, unsilencing of AMPAR-silent synapses has been implicated in various neurodevelopmental disorders (Hanse et al., 2013). Interestingly, GluA4 -/- mice exhibit some aspects of schizophrenia-related phenotypes (Sagata et al., 2010). However, whether these phenotypes are due to perturbed glutamatergic development or adult phenotype involving reduced excitatory drive onto parvalbumin-positive fast-spiking interneurons (Fuchs et al., 2007), remains to be elucidated.

Molecular mechanism underlying PKA–driven synaptic insertion of GluA4

We identified two critical CTD sequences regulating PKA-dependent synaptic insertion of GluA4 in immature CA1 pyramidal neurons: the membrane proximal region (MPR) (835-869) and the extreme C-terminal amino acids. The MPR has been previously implicated in GluA4 trafficking (Boehm et al., 2006) and incorporates the established interaction sites for the protein 4.1N (Coleman et al., 2003), PKCγ (Correia et al., 2003), α-actinin-1 and IQGAP1 (Nuriya et al., 2005). The MPR sequence has been reported to promote GluA4 surface expression (Carvalho et al., 1999; Coleman et al., 2003; Gomes et al., 2007; Zheng and Keifer, 2008; 2014) as well as phosphorylation by PKCγ at Ser862 (Gomes et al., 2007). However, using a RKR/SSS mutant to selectively knock out 4.1N and PKCg interactions, we found that these proteins alone are not sufficient for PKA-dependent synaptic delivery of GluA4 at immature CA3-CA1 synapses. This suggests that PKA- and PKC–dependent signaling pathways may employ separate molecular mechanisms to regulate GluA4 trafficking and leaves a-actinin-1 and IQGAP as the potential relevant interactors for PKA–dependent synaptic insertion.

It has been suggested that α-actinin-1 keeps GluA4 in the intracellular pool and, upon synaptic activity and GluA4 phosphorylation, this binding to α-actinin-1 is disrupted to allow GluA4 incorporation into synapses (Nuriya et al., 2005). In our experiments the phosphorylation status of Ser862 did not influence the ability of GST-A4 CTD protein to regulate forskolin-induced insertion of GluA4, suggesting that another mechanism independent of the Ser862 phosphorylation is also involved.

Interestingly, and unexpectedly, mutation or deletion of the extreme C-terminal residues of GluA4 completely abolished the ability of GST-A4 CTD to block forskolin-induced potentiation. No functional role for the extreme C-terminal region of GluA4 has yet been proposed. This region is similar to the PDZ binding motif critically involved in GluA1 trafficking but blocked with an extra proline residue (Hayashi et al., 2000; Malinow and Malenka, 2002; Coleman et al., 2010). However, the extreme C-terminal sequence alone was not sufficient to regulate GluA4 trafficking, as GST-A4(870-902) had no effect. To reconcile these findings, we may assume that the C-terminal region, even if it did not directly participate in the mechanisms underlying the forskolin-dependent potentiation, would have a facilitatory influence on the ability of the MPR to interact with the critical protein(s). This influence would be removed by C-terminal mutations explaining the loss of activity, whereas the MPR (the segment 835–869), when expressed in the absence of further C-terminal sequences, would assume an active conformation (Figure 5). In the absence of structural data on GluA4 CTD, the physical nature of this influence cannot be established, but based on the activities of wild-type and mutated CTD peptides, it is likely to involve an interaction between the MPR and the C-terminal half of the CTD. We propose a scenario in which the extreme C-terminal residues play an essential role in keeping the C-terminal half of GluA4 CTD in a “closed state”, which stabilizes the critical protein interaction(s) of the MPR. C-terminal mutations would prevent the formation of this closed state and the resulting alternative structure would prevent the MPR form adopting a conformation compatible with protein interactions. Such a co-operative role of the C-terminal half

is also consistent with the finding that CTD peptide 835-869, lacking the the C-terminal half of CTD, inhibits the forskolin-dependent GluA4 insertion like the full-length CTD peptide.

To further understand the importance of the identified sites for GluA4 trafficking, we studied the distribution of GFP-tagged GluA4 with different CTD mutations in hippocampal cell culture. As reported earlier (Zhu et al., 2000; Coleman et al., 2003; Esteban et al., 2003; Coleman et al., 2006), GFP-GluA4 was transported to dendrites and was readily delivered to the surface of hippocampal neurons in culture. Consistent with a critical role of the MPR in trafficking, GFP-GluA4 lacking MPR was completely restricted to the soma, most likely trapped in the endoplasmic reticulum. Both dendritic delivery and synaptic recruitment of GFP-GluA4 with deletion of the extreme C-terminal sequence were significantly diminished as compared to wild type GFP-GluA4, while the RKR/SSS mutant behaved similar to the WT.

Together, these data confirm a critical role for the MPR in trafficking of GluA4 and identify a novel contribution by the extreme C-terminal region to activity dependent synaptic delivery of GluA4. The molecular identity of the proteins interacting with these regions to regulate PKA-dependent trafficking of GluA4 cannot be resolved based on our data. Rather, our data suggest that a yet unidentified interacting protein and/or interactions between the extreme C-terminal region and the MPR regulate PKA-dependent trafficking of GluA4 at immature hippocampal CA3-CA1 synapses.

Acknowledgements: This work was supported by the Academy of Finland, Sigrid Juselius foundation, the Finnish Graduate School of Neuroscience and Finnish Cultural Foundation. We thank Kirsi Ahde for her assistance with work involving cell cultures.

References

Anderson WW, Collingridge GL (2001) The LTP Program: a data acquisition program for on-line analysis of long-term potentiation and other synaptic events. J Neurosci Methods 108:71-83.

Anggono V, Huganir RL (2012) Regulation of AMPA receptor trafficking and synaptic plasticity. Curr Opin Neurobiol 22: 461-469.

Bassani S, Folci A, Zapata J, Passafaro M(2013) AMPAR trafficking in synapse maturation and plasticity. Cell Mol Life Sci 70: 4411-4430.

Boehm J, Kang M-G, Johnson RC, Esteban J, Huganir RL, Malinow R (2006) Synaptic incorporation of AMPA receptors during LTP is controlled by a PKC phosphorylation site on GluR1. Neuron 51: 213-225.

Carvalho AL, Kameyama K, Huganir RL (1999) Characterization of phosphorylation sites on the glutamate receptor 4 subunit of the AMPA receptors. J Neurosci 19: 4748-4754.

Coleman SK, Cai C, Kalkkinen N, Korpi ER, Keinänen K (2010) Analysis of the potential role of GluA4 carboxyl-terminus in PDZ interactions. PLoS One 5: e8715.

Coleman SK, Möykkynen T, Cai C, von Ossowski L, Kuismanen E, Korpi ER, Keinänen K (2006) Isoform-specific early trafficking of AMPA receptor flip and flop variants. J Neurosci 26: 11220-11229.

Coleman, SK, Cai C, Mottershead DG, Haapalahti J-P, Keinänen K (2003) Surface expression of GluR-D AMPA receptor is dependent on an interaction between its C-terminal domain and a 4.1 protein. J Neurosci 23: 798-806.

Correia SS, Duarte CB, Faro CJ, Pires EV, Carvalho AL (2003) Protein kinase C gamma associates directly with the GluR4 alpha-amino-3-hydroxy-5-methyl-4-isoxazole propionate receptor subunit. Effect on receptor phosphorylation. J Biol Chem 278: 6307-6313.

Crair MC, Malenka RC (1995) A critical period for long-term potentiation at thalamocortical synapses. Nature 375: 325-328.

Durand GM, Kovalchuk Y, Konnerth A (1996) Long-term potentiation and functional synapse induction in developing hippocampus. Nature 381: 71-75.

Elias GM, Funke L, Stein V, Grant SG, Bredt DS, Nicoll RA (2006) Synapse-specific and developmentally regulated targeting of AMPA receptors by a family of MAGUK scaffolding proteins. Neuron 52: 307-320.

Esteban JA, Shi S-H, Wilson C, Nuriya M, Huganir RL, Malinow R (2003) PKA phosphorylation of AMPA receptor subunits controls synaptic trafficking underlying plasticity. Nat Neurosci 6: 136-143.

Fiala JC, Feinberg M, Popov V, Harris KM (1998) Synaptogenesis via dendritic filopodia in developing hippocampal area CA1. J Neurosci 18: 8900-8911.

Fuchs EC, Zivkovic AR, Cunningham MO, Middleton S, Lebeau FEN, Bannerman DM, Rozov A, Whittington MA, Traub RD, Rawlins JNP, Monyer H (2007) Recruitment of parvalbumin-positive interneurons determines hippocampal function and associated behavior. Neuron 53: 591-604.

Geiger JR, Melcher T, Koh DS, Sakmann B, Seeburg PH, Jonas P, Monyer H (1995) Relative abundance of subunit mRNAs determines gating and Ca2+ permeability of AMPA receptors in principal neurons and interneurons in rat CNS. Neuron 15:193–204.

Gomes AR, Correia SS, Esteban JA, Duarte CB, Carvalho AL (2007) PKC anchoring to GluR4 AMPA receptor subunit modulates PKC-driven receptor phosphorylation and surface expression. Traffic 8: 259-269.

Granger AJ, Shi Y, Lu W, Cerpas M, Nicoll RA (2013) LTP requires a reserve pool of glutamate receptors independent of subunit type. Nature 493: 495-500.

Hanse E, Seth H, Riebe I (2013) AMPA-silent synapses in brain development and pathology. Nat Rev Neurosci 14: 839-850.

Hanse E, Taira T, Lauri S, Groc L (2009) Glutamate synapse in developing brain: an integrative perspective beyond the silent state. Trends Neurosci 32: 532-537.

Häusser M, Roth A (1997) Estimating the time course of the excitatory synaptic conductance in neocortical pyramidal cells using a novel voltage jump method. J Neurosci. 17(20):7606-25.

Hayashi Y, Shi SH, Esteban JA, Piccini A, Poncer JC, Malinow R (2000) Driving AMPA receptors into synapses by LTP and CaMKII: requirement for GluR1 and PDZ domain interaction. Science 287: 2262-2267.

Ho MT, Pelkey KA, Topolnik L, Petralia RS, Takamiya K, Xia J, Huganir RL, Lacaille JC, McBain CJ (2007) Developmental expression of Ca2+-permeable AMPA receptors underlies depolarization-induced long-term depression at mossy fiber CA3 pyramid synapses. J Neurosci 27:11651–11662.

Hsia AY, Malenka RC, Nicoll RA (1998) Development of excitatory circuitry in the hippocampus. J Neurophysiol 79: 2013-2024.

Huupponen J, Molchanova SM, Taira T, Lauri SE (2007) Susceptibility for homeostatic plasticity is down-regulated in parallel with maturation of the rat hippocampal synaptic circuitry. J Physiol 581: 505-514.

Isaac JT, Hjelmstad GO, Nicoll RA, Malenka RC (1996) Long-term potentiation at single fiber inputs to hippocampal CA1 pyramidal cells. Proc Natl Acad Sci U S A 93: 8710-8715.

Kerchner GA, Nicoll RA (2008) Silent synapses and the emergence of a postsynaptic mechanism for LTP. Nat Rev Neurosci 9: 813-825.

Kumar SS, Bacci A, Kharazia V, Huguenard VR (2002) A developmental switch of AMPA receptor subunits in neocortical pyramidal neurons. J Neurosci 22: 3005–3015.

Li H, Khirug S, Cai C, Ludwig A, Blaesse P, Kolikova J, Afzalov R, Coleman SK, Lauri S, Airaksinen MS, Keinänen K, Khiroug L, Saarma M, Kaila K, Rivera C (2007) KCC2 interacts with the dendritic cytoskeleton to promote spine development. Neuron 56: 1019-1033.

Lu HC, Gonzalez E, Crair MC (2001) Barrel cortex critical period plasticity is independent of changes in NMDA receptor subunit composition. Neuron 32: 619-634.

Luchkina NV, Huupponen J, Clarke VRJ, Coleman SK, Keinänen K, Taira T, Lauri SE (2014) Developmental switch in the kinase dependency of long-term potentiation depends on expression of GluA4 subunit-containing AMPA receptors. Proc Natl Acad Sci U S A 111: 4321-4326.

Malinow R, Malenka RC (2002) AMPA receptor trafficking and synaptic plasticity. Annu Rev Neurosci 25: 103-126.

Monyer H, Seeburg PH, Wisden W (1991) Glutamate-operated channels: developmentally early and mature forms arise by alternative splicing. Neuron 6(5):799-810.

Mosbacher J, Schoepfer R, Monyer H, Burnashev N, Seeburg PH, Ruppersberg JP (1994) A molecular determinant for submillisecond desensitization in glutamate receptors. Science 266:1059–1062.

Nuriya M, Oh S, Huganir RL (2005) Phosphorylation-dependent interactions of alpha-Actinin-1/IQGAP1 with the AMPA receptor subunit GluR4. J Neurochem 95: 544-552.

Opazo P, Choquet DA (2011) three-step model for the synaptic recruitment of AMPA receptors. Mol Cell Neurosci 46: 1-8.

R Core Team (2014) R: A language and environment for statistical computing. R Foundation for Statistical Computing, Vienna, Austria. http://www.R-project.org/

Sagata N, Iwaki A, Aramaki T, Takao K, Kura S, Tsuzuki T, Kawakami R, Ito I, Kitamura T, Sugiyama H, Miyakawa T, Fukumaki Y (2010) Comprehensive behavioural study of GluR4 knockout mice: implication in cognitive function. Genes Brain Behav 9: 899-909.

Saviane C, Savtchenko LP, Raffaelli G, Voronin LL, Cherubini E (2002) Frequency-dependent shift from paired-pulse facilitation to paired-pulse depression at unitary CA3-CA3 synapses in the rat hippocampus. J Physiol 544: 469-476

Schmitz SK, Hjorth JJJ, Joemai RMS, Wijntjes R, Eijgenraam S, de Bruijn P, Georgiou C, de Jong APH, van Ooyen A, Verhage M, Cornelisse LN, Toonen RF, Veldkamp WJH, Veldkamp W (2011) Automated analysis of neuronal morphology, synapse number and synaptic recruitment. J Neurosci Methods 195: 185-193.

Schneider CA, Rasband WS, Eliceiri KW (2012) NIH Image to ImageJ: 25 years of image analysis. Nat Methods 9: 671-675.

Stevens CF, Wang Y (1995) Facilitation and depression at single central synapses. Neuron 14: 795-802.

Swanson GT, Kamboj SK, Cull-Candy SG (1997) Single-channel properties of recombinant AMPA receptors depend on RNA editing, splice variation, and subunit composition. J Neurosci 17: 58-69.

Voronin LL, Cherubini E (2004) 'Deaf, mute and whispering' silent synapses: their role in synaptic plasticity. J Physiol 557: 3-12.

Xiao M-Y, Wasling P, Hanse E, Gustafsson B (2004) Creation of AMPA-silent synapses in the neonatal hippocampus. Nat Neurosci 7: 236-243.

Yasuda H, Barth AL, Stellwagen D, Malenka RC (2003) A developmental switch in the signaling cascades for LTP induction. Nat Neurosci 6: 15-16.

Ye G-L, Yi S, Gamkrelidze G, Pasternak JF, Trommer BL (2005) AMPA and NMDA receptor-mediated currents in developing dentate gyrus granule cells. Brain Res Dev Brain Res 155: 26-32.

Zheng Z, Keifer J (2008) Protein kinase C-dependent and independent signaling pathways regulate synaptic GluR1 and GluR4 AMPAR subunits during in vitro classical conditioning. Neuroscience 156: 872-884.

Zheng Z, Keifer J (2014) Sequential delivery of synaptic GluA1- and GluA4-containing AMPA receptors (AMPARs) by SAP97 anchored protein complexes in classical conditioning. J Biol Chem 289: 10540-10550.

Zhu JJ (2009) Activity level-dependent synapse-specific AMPA receptor trafficking regulates transmission kinetics. J Neurosci. 29(19):6320-35.

Zhu JJ, Esteban JA, Hayashi Y, Malinow R (2000) Postnatal synaptic potentiation: delivery of GluR4-containing AMPA receptors by spontaneous activity. Nat Neurosci 3: 1098-1106.

FIGURES

1. PKA activation leads to insertion of GluA4 to immature synapses with initially weak or silent AMPA transmission

    A. Single example illustrating the experimental protocol to study the AMPA (-70 mV) and NMDA currents (+40mV, slow component) in response to minimal stimulation and the effect of forskolin in a WT slice. Averaged EPSCs (15 responses including failures) from time points indicated are shown on the top. The bar graphs show pooled data on the relative average amplitude (forskolin to baseline) as well as potency and success rate before and after forskolin application for AMPA and NMDA EPSCs, at immature CA3-CA1 synapses (P4-P8) (n=9).
    B. Corresponding data for GluA4-/- mice (n=9). * $p<0.05$

2. Delayed maturation of AMPAR-mediated transmission in the absence of GluA4

    A. Age-dependent changes of AMPA/NMDA ratio in WT (n=61) vs. GluA4 -/- mice (n=76). Sigmoid function fitting showed as a dotted line.
    B. Pooled data comparing the AMPA/NMDA ratio between WT and GluA4-/- mice in different age groups. Examples of averaged EPSCs recorded at -70 mV and at +40 mV are shown on the left. * $p<0.05$
    C. Example traces and cumulative plots depicting frequency and amplitude of mEPSCs in CA1 pyramidal neurons of WT (n=8) and GluA4-/- (n=12) mice at P10-P11.

3. The membrane proximal region and the extreme C-terminal sequences of GluA4 CTD are critical for PKA-dependent synaptic potentiation

    A. The sequences of the GluA4 CTD protein constructs used. The characterized protein interaction sites as well as the Ser862 phosphorylation site are indicated in the WT CTD sequence on the top row (A4(835-902)).
    B. Time course plots showing the effect of forskolin on EPSCs, with various GST-A4 CTD proteins infused to the recorded cell via the patch electrode. Superimposed example traces before and after forskolin application are shown on top and pooled data with denoted statistical significance on the right. GST-A4(870-902) (n=6), GST-A4(835-869) (n=12), * $p<0.05$.
    C. Corresponding data for GST–A4(835-902,S862A)(n=9), GST–A4(835-902,S862D)(n=7) and GST–A4(835-902,RKR/SSS) (n=10).
    D. Corresponding data for GST–A4(835-896) (n=6), GST–A4(835-901, L901A) (n=7) and GST-A4(835-901)(n=7).

4. The membrane proximal region and extreme C-terminal sequences regulate dendritic delivery, synaptic targeting and surface expression of GluA4 in hippocampal neurons

   A. Confocal images of cultured hippocampal neurons expressing full-length GFP-tagged GluA4 (GFP-A4(22-902)), GFP-A4(22-902,RKR/SSS) with disrupted protein 4.1 and PKCγ interaction site, GFP-A4(22-896) with deletion of extreme C-terminal region, and GFP-A4(22-837, 870-902) where the membrane proximal region has been deleted. Removal of MPR of the GluA4 CTD leads to accumulation of the construct in neuronal cell body. anti-MAP2 staining (blue), anti-GFP surface staining (red). Scale bar 25 μm.
   B. Confocal images of cells expressing GFP, GFP-A4(22-902), GFP-A4(22-902,RKR/SSS) and GFP-A4(22-896). The neurons have been surface stained for GFP (red) and, after permeabilization, for PSD95 (blue). Scale bar 25 μm for images of cells, 5 μm for insets of dendrites.
   C. Pooled data on the dendritic delivery, synaptic recruitment and synaptic surface expression of the various constructs. GFP-A4(22-902) (n=19), GFP-A4(22-902,RKR/SSS) (n=12), GFP-A4(22-896) (n=14) from at least 3 independent neuronal cultures. * $p<0.05$.

5. A hypothetical model on the role of the extreme c-terminal sequence in GluA4 synaptic recruitment.

   A. Synaptic recruitment of GluA4 is facilitated by an active CTD conformation which enables binding of MPR (purple) to critical protein(s) (yellow hexagon). This conformation is stabilized by interaction of the extreme c-terminal region (black) with the MPR.
   C. The full-length GST-A4 CTD fusion proteins inhibit synaptic recruitment of GluA4 by scavenging endogenous proteins interacting with the MPR. The GST-A4(835-869) assumes an active conformation, and thus is able to scavenge the interacting proteins, while the c-terminal half alone has no effect. The mutations in the extreme c-terminal region stabilize an inactive conformation, unable to bind the putative interacting proteins.
   D. The recombinant GFP-tagged GluA4 constructs lacking the MPR or the c-terminal amino-acids show impaired trafficking in cultured neurons because of inability (GFP A4(22-837;870-902) or reduced ability (GFP A4(22-896) to interact with the critical MPR binding proteins. Green dot represents GFP protein.

Figure 1

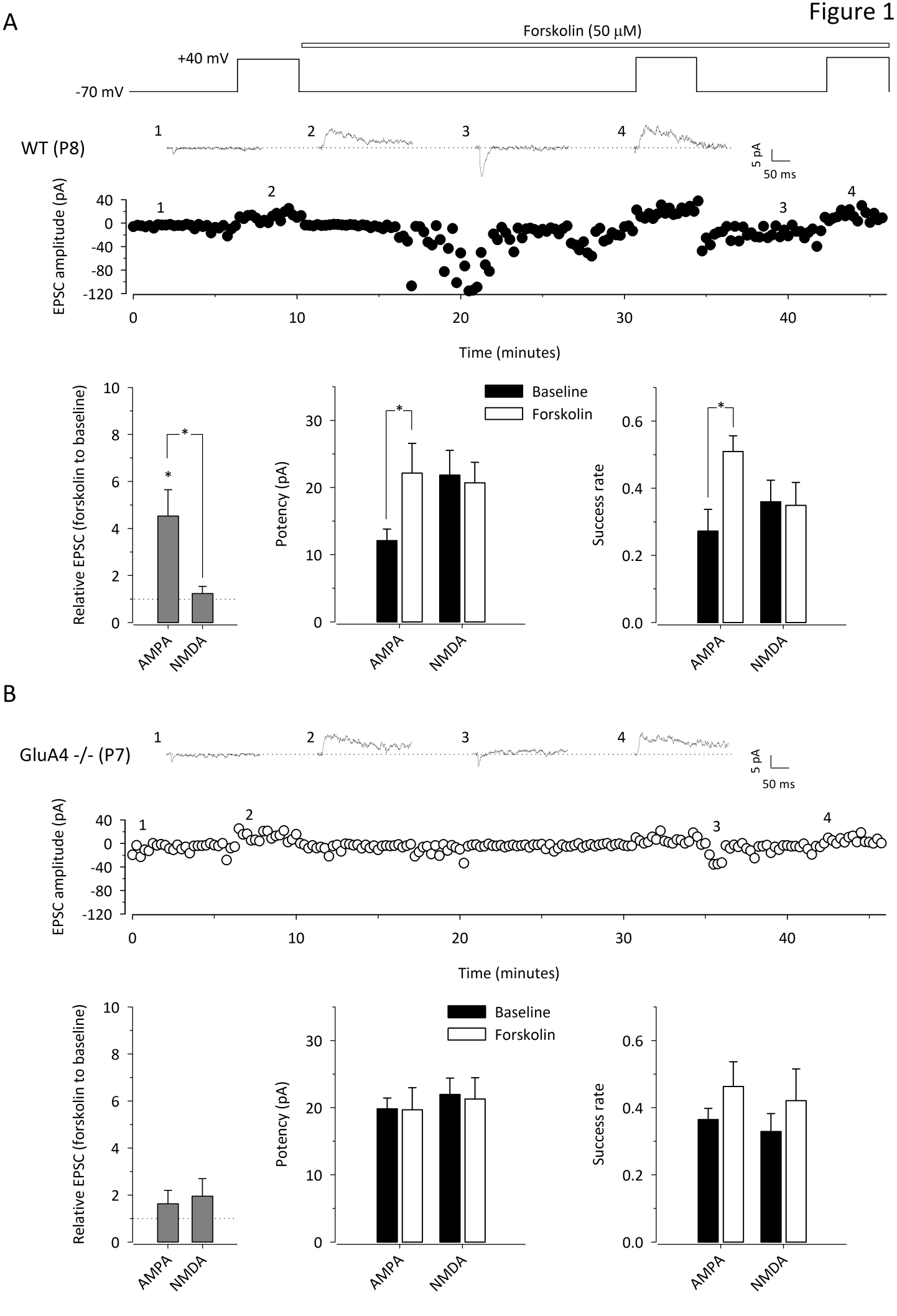
A
Forskolin (50 μM)
+40 mV
-70 mV
WT (P8)
1
2
3
4
5 pA
50 ms
EPSC amplitude (pA)
40
0
-40
-80
-120
0
10
20
30
40
Time (minutes)
Relative EPSC (forskolin to baseline)
10
8
6
4
2
0
*
*
AMPA
NMDA
Potency (pA)
30
20
10
0
Baseline
Forskolin
*
AMPA
NMDA
Success rate
0.6
0.4
0.2
0.0
*
AMPA
NMDA
B
GluA4 -/- (P7)
1
2
3
4
5 pA
50 ms
EPSC amplitude (pA)
40
0
-40
-80
-120
0
10
20
30
40
Time (minutes)
Relative EPSC (forskolin to baseline)
10
8
6
4
2
0
AMPA
NMDA
Potency (pA)
30
20
10
0
Baseline
Forskolin
AMPA
NMDA
Success rate
0.6
0.4
0.2
0.0
AMPA
NMDA

Figure 2

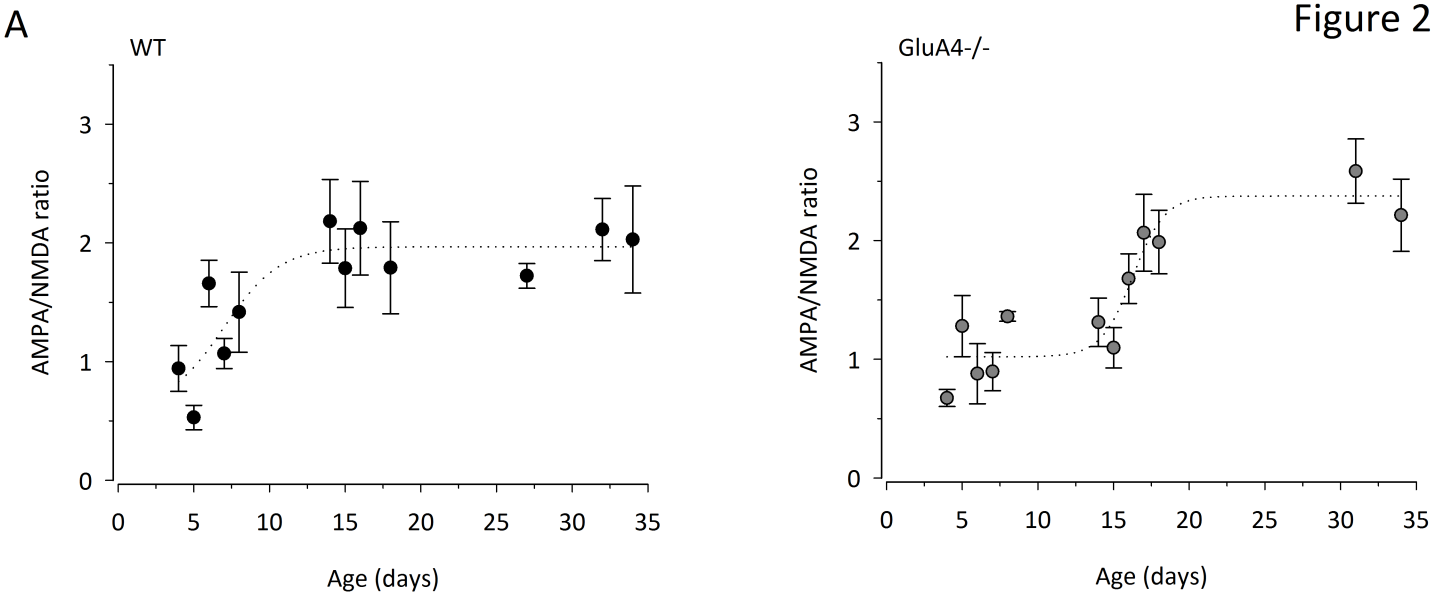
A
WT
GluA4-/-
AMPA/NMDA ratio
Age (days)
0
1
2
3
0
5
10
15
20
25
30
35

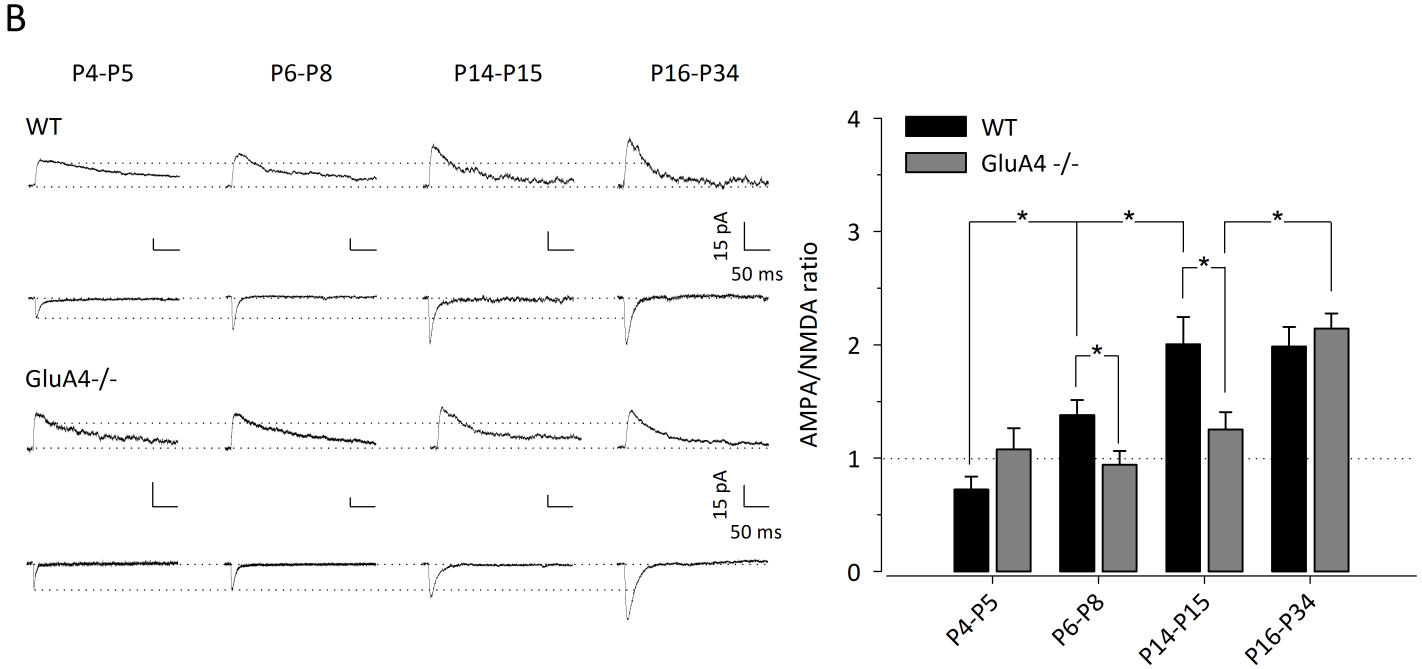
B
P4-P5
P6-P8
P14-P15
P16-P34
WT
GluA4-/-
15 pA
50 ms
AMPA/NMDA ratio
WT
GluA4 -/-
*
P4-P5
P6-P8
P14-P15
P16-P34

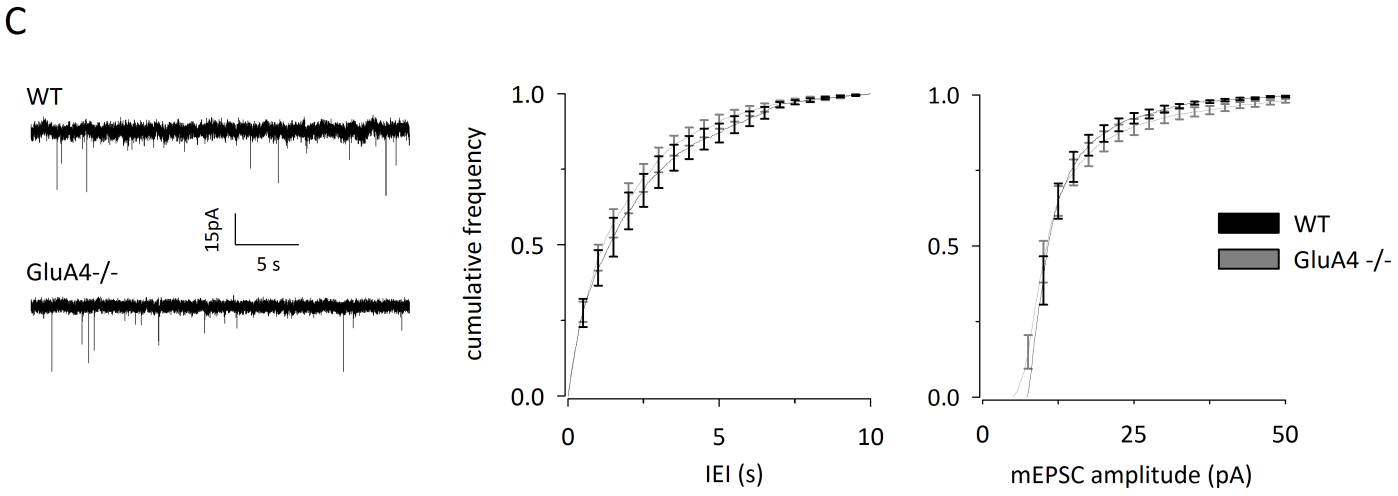
C
WT
GluA4-/-
15pA
5 s
cumulative frequency
IEI (s)
mEPSC amplitude (pA)
WT
GluA4 -/-

Figure 3

A

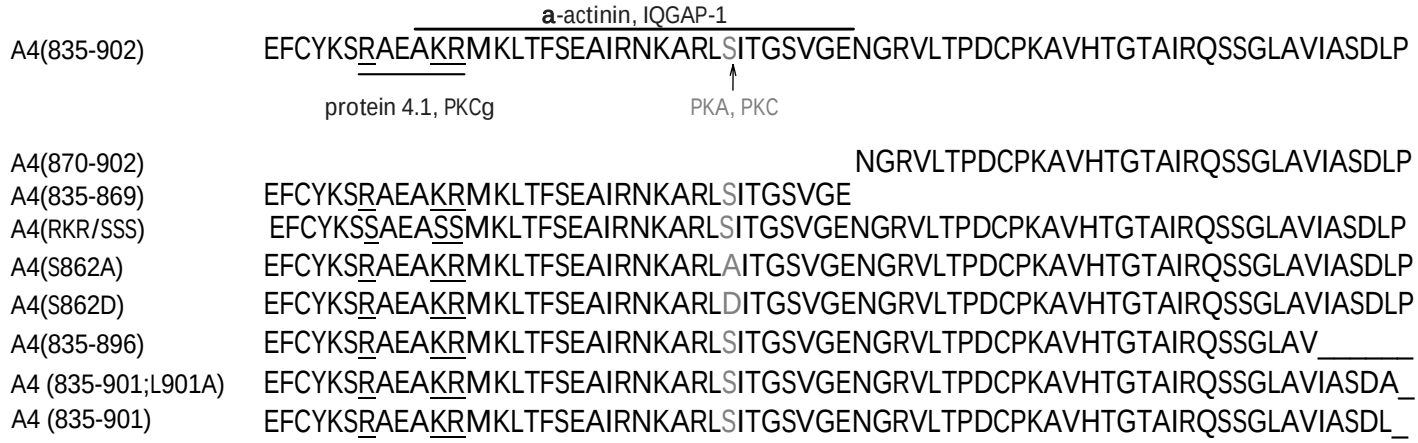

B

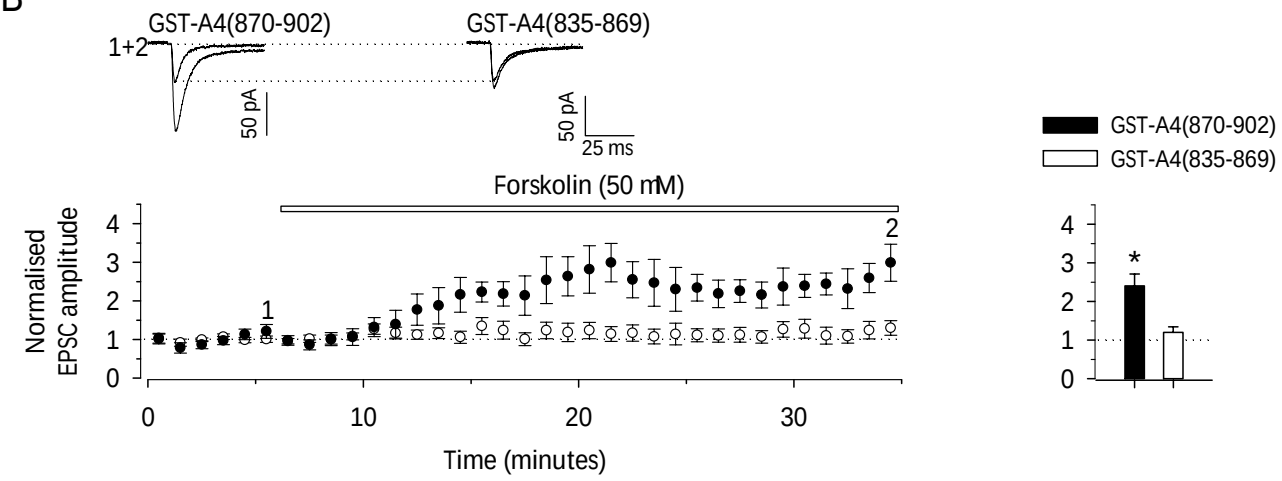

C

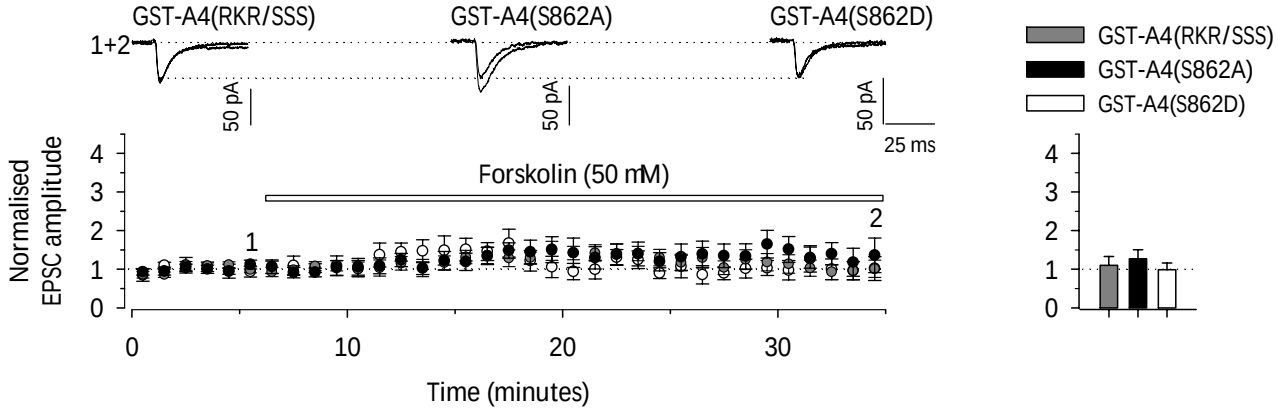

D

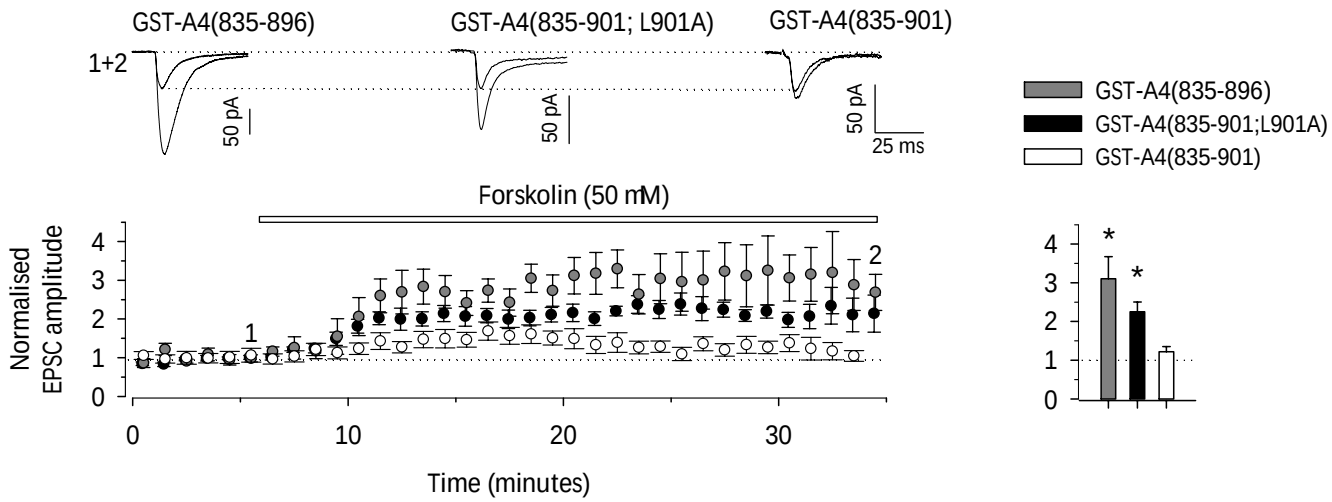

Figure 4

A

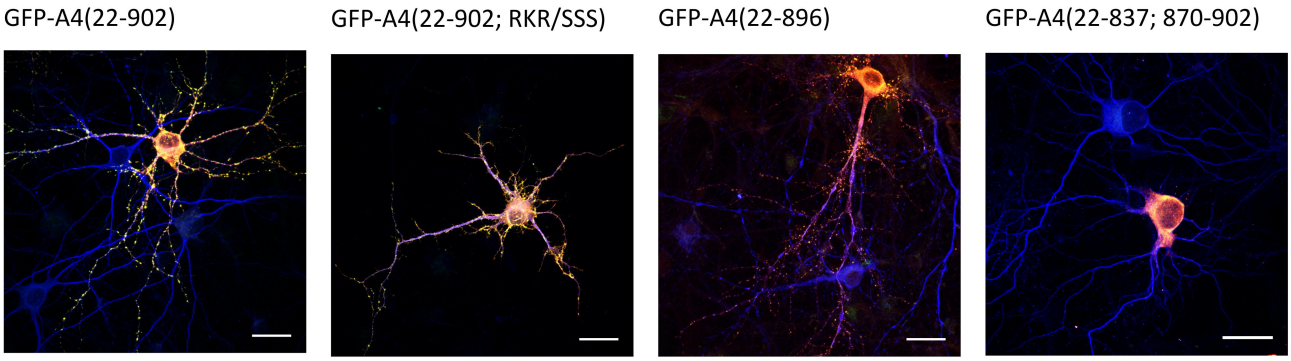
GFP-A4(22-902)
GFP-A4(22-902; RKR/SSS)
GFP-A4(22-896)
GFP-A4(22-837; 870-902)

B

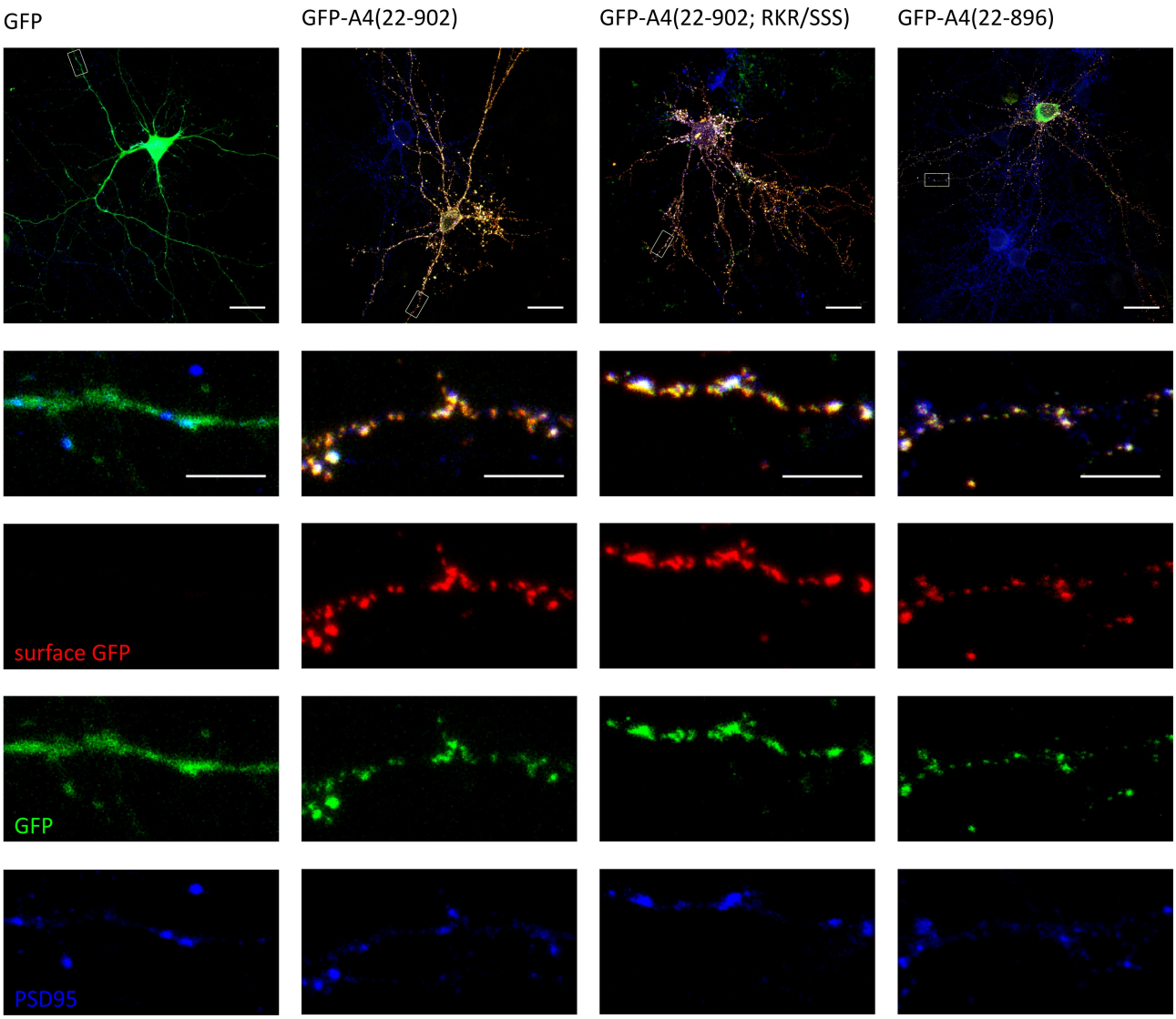
GFP
GFP-A4(22-902)
GFP-A4(22-902; RKR/SSS)
GFP-A4(22-896)
surface GFP
GFP
PSD95

C

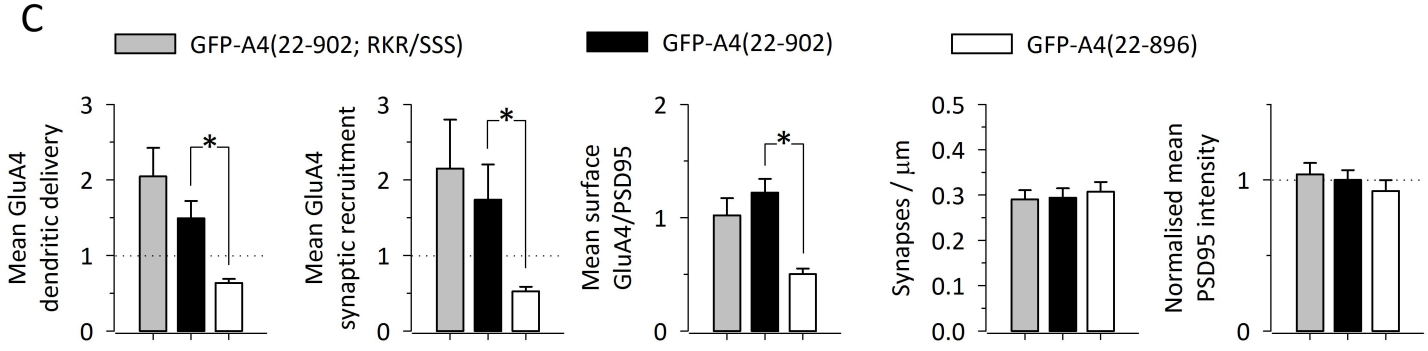
GFP-A4(22-902; RKR/SSS)
GFP-A4(22-902)
GFP-A4(22-896)
Mean GluA4 dendritic delivery
Mean GluA4 synaptic recruitment
Mean surface GluA4/PSD95
Synapses / µm
Normalised mean PSD95 intensity
*

Figure 5

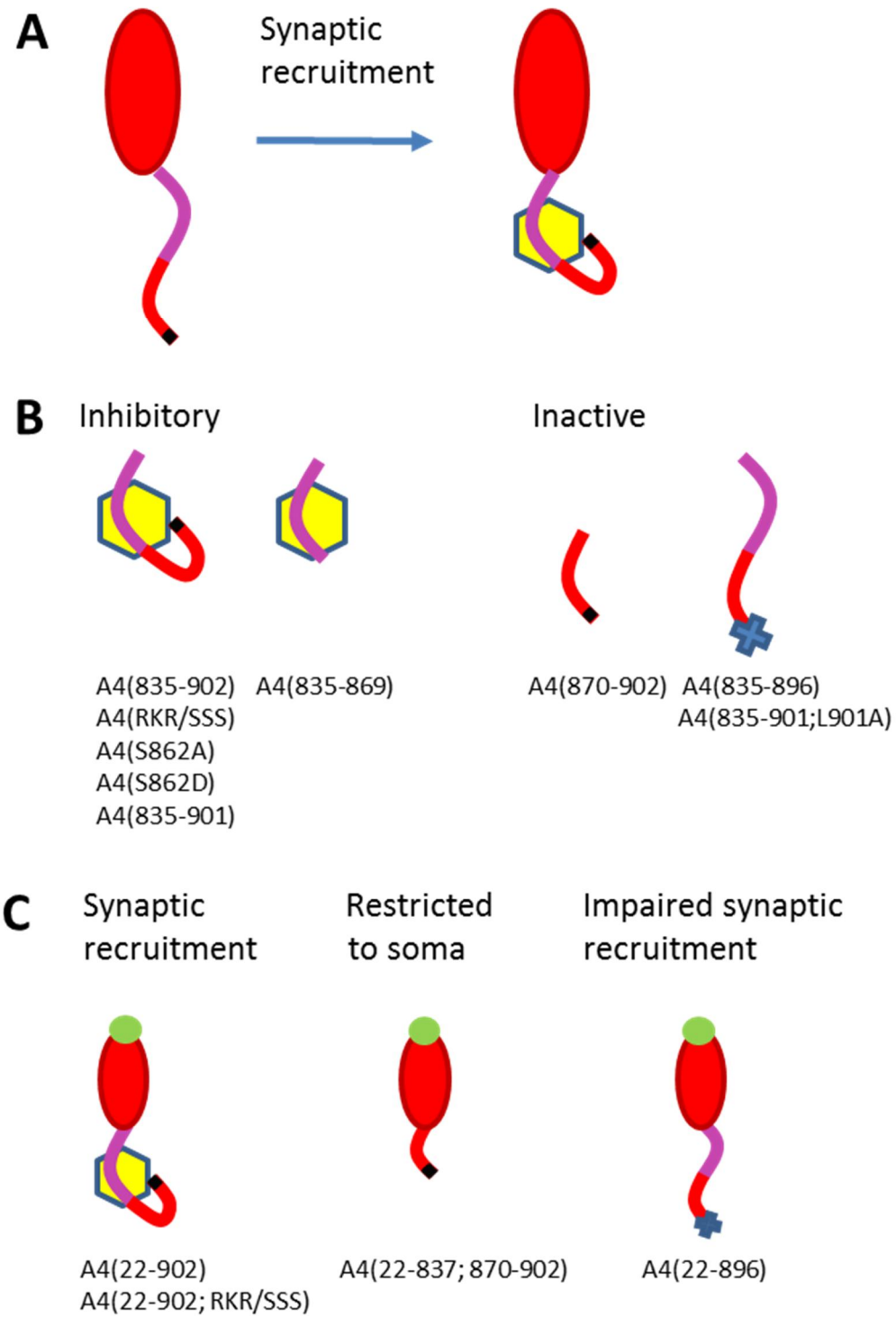
A
Synaptic recruitment
B
Inhibitory
Inactive
A4(835-902)
A4(RKR/SSS)
A4(S862A)
A4(S862D)
A4(835-901)
A4(835-869)
A4(870-902)
A4(835-896)
A4(835-901;L901A)
C
Synaptic recruitment
Restricted to soma
Impaired synaptic recruitment
A4(22-902)
A4(22-902; RKR/SSS)
A4(22-837; 870-902)
A4(22-896)